ELSEVIER

Journal of Chromatography A, 905 (2001) 269–279

JOURNAL OF CHROMATOGRAPHY A

www.elsevier.com/locate/chroma

Optimization of background electrolytes for capillary electrophoresis I. Mathematical and computational model

Bohuslav Gaš*, Pavel Coufal, Michal Jaroš, Jan Muzikář, Ivan Jelínek

Faculty of Science, Charles University, Albertov 2030, CZ-128 40 Prague 2, Czech Republic

Received 15 June 2000; received in revised form 22 August 2000; accepted 21 September 2000

Abstract

A mathematical and computational model is introduced for optimization of background electrolyte systems for capillary zone electrophoresis of anions. The model takes into account mono- or di- or trivalent ions and allows also for modeling of highly acidic or alkaline electrolytes, where a presence of hydrogen and hydroxide ions is significant. At maximum, the electrolyte can contain two co-anions and two counter-cations. The mathematical relations of the model are formulated to enable an easy algorithmization and programming in a computer language. The model assesses the composition of the background electrolyte in the analyte zone, which enables prediction of the parameters of the system that are experimentally available, like the transfer ratio, which is a measure of the sensitivity in the indirect photometric detection or the molar conductivity detection response, which expresses the sensitivity of the conductivity detection. Furthermore, the model also enables the evaluation of a tendency of the analyte to undergo electromigration dispersion and allows the optimization of the composition of the background electrolyte to reach a good sensitivity of detection while still having the dispersion properties in the acceptable range. Although the model presented is aimed towards the separation of anions, it can be straightforwardly rearranged to serve for simulation of electromigration of cationic analytes. The suitability of the model is checked by inspecting the behavior of a phosphate buffer for analysis of anions. It is shown that parameters of the phosphate buffer when used at neutral and alkaline pH values possess singularities that indicate a possible occurrence of system peaks. Moreover, if the mobility of any analyte of the sample is close to the mobilities of the system peaks, the indirect detector signals following the background electrolyte properties will be heavily amplified and distorted. When a specific detector sensitive on presence of the analyte were used, the signal would be almost lost due to the excessive dispersion of the peak.

Keywords: Mathematical modelling; Optimization; Background electrolyte composition

1. Introduction

Unlike separation in chromatography which is mostly performed in the linear regimen, the separation process in capillary electrophoresis is of inherently nonlinear nature. This feature of capillary electrophoresis makes it difficult to design properly the separation systems and to understand possible disturbing phenomena.

Electromigration dispersion in capillary zone electrophoresis (CZE) is one of the deteriorating phenomena which is a consequence of the nonlinearity. It causes peak dispersion and various deformations of peak shapes and significantly decreases the sepa-

*Corresponding author. Tel.: +420-2-2195-2437; fax: +420-2-2491-9752.

E-mail address: gas@natur.cuni.cz (B. Gaš).

0021-9673/01/$ – see front matter
PII: S0021-9673(00)00983-3

ration efficiency. When the resolution of the separation is sufficient, the electromigration dispersion does not deteriorate the analysis but simply broadens the peaks. However, in many analyses of practical importance there is an analyte in a relatively small concentration which is accompanied by a matrix with a much higher concentration. Here the excessively dispersing peak of the matrix can conceal the analyte peak and disable its detection.

Various electrolyte systems have a various tendency to cause electromigration dispersion. If indirect photometric detection is to be utilized, often the background electrolyte (BGE) contains two co-ions: one of them is light-absorbing and the second one has more appropriate acido–basic properties for the particular system [1,2]. Although at first glance this might seem to be the most convenient configuration for the purposes of indirect detection, the systems with multiple co-ions cause unexpected phenomena. Analogous phenomena connected with indirect detection were earlier noticed in chromatographic separation and were analyzed by Poppe [3,4]. He explained the existence of new system peaks, which he called ''eigenpeaks'' and also derived that the response of an indirect detector tends to reach ±infinity, when the retention of an analyte peak draws near the retention of the eigenpeak. Unlike the ''normal water gap'' peak, which is caused by a jump in the Kohlrausch regulating function, and which moves in the column only due to the electroosmotic flow, the system eigenpeaks have a certain electrophoretic velocity. Their behavior has been investigated by many authors [5–10]. It was further noticed that also other macroscopic properties of the background electrolytes like the velocity slope, which is a measure of the electromigration dispersion can attain ±infinity under certain conditions. This can cause severe broadening of the analyte peak [11–14], which was named ''schizophrenic'' broadening by Gebauer et al. [15]. Recently it was pointed out by Boček et al. [16] that even electrolytes with higher valency of ions like phosphate buffers when used in the pH region where two ionic forms are present (e.g. at pH~7) cause unexpected broadening of the analyte peaks.

To reveal the behavior of the analytes during the electrophoretic separation, it is necessary to get an insight into a complete composition of the BGE in the sample zone, when a sample migrates by electromigration movement through the BGE. Furthermore, knowledge of this composition enables inspection of the macroscopic properties of the electrolyte which can be obtained by detectors like, e.g. direct or indirect photometric detectors and conductivity detectors and to assess the sensitivity of detection.

The theoretical model allowing calculation of complete composition of the BGE in the sample zone was earlier completely solved for zones migrating in the isotachophoretic (ITP) steady state mode [17]. For zone electrophoresis the attempts to calculate composition of the sample zones are more recent. Beckers interestingly employed the multiple use of the ITP steady state model for calculation of the electrolyte composition in the CZE zone [18–21]. Gebauer et al. [22,23] proposed another mathematical model for the calculation of sample zone composition and used it for predicting peak shapes distorted by electromigration dispersion. The composition in the sample CZE zone was also calculated by Xiong and Li [24] who determined the analytical sensitivity of indirect UV detection both in electrolyte systems with absorbing co-ions and counterions. A simple model for calculating concentration distribution, which allows the use of spreadsheet programs for calculation, was proposed by Mikkers [25].

When examining the models for calculation of the zone composition used by various authors, they all use the same basic relations: electroneutrality condition, mass balance or continuity equations, equations describing dissociation equilibria and most of them use also the Kohlrausch regulating function [26]. The pH range of applicability of the models is different and most of them can be used only for the ''safe'' pH region, i.e. where concentration of H^+ ions and mainly their contribution to the current and mass transport, is much smaller than that of the other ions. As the mobility of H^+ ions is considerably high so they contribute much to the transport, the safe region for 10 m*M* electrolyte solutions is rather narrow, pH 4.5–9.5. Here contribution of the H^+ ions to the transport of current is less than 10%. The original form of the Kohlrausch regulating function cannot be used for the pH range lying beyond the

safe region, which was nicely discussed by Ermakov et al. [27]. Therefore Gebauer et al., whose model [22,15] is applicable for the strongly acidic pH range, used a rather complicated correction term in the regulating function to appropriately describe the behavior of the system. Previously, we have derived an extended form [28] of the regulating function, which is valid for weak uni-univalent electrolytes with a significant content of hydrogen or hydroxide ions and which brings a substantial simplification to the description of the behavior of such systems. Such a form of the Kohlrausch regulating function was recently used by Gebauer et al. [29], who have shown that in highly acidic and alkaline BGEs the H^+ and OH^- ions form other co-ions for separations of cations and anions, respectively, with all consequences of using electrolytes with multiple co-ions.

From what is stated above it is obvious that some characteristics of the BGEs like sensitivity of detection, are desirable and should be kept high while there are also deteriorating features like electromigration dispersion or occurrence of system peaks, which should be suppressed. If a theoretical model describing the behavior of the electrolyte is correctly proposed, it enables prediction of those features and allows optimization of the composition of the BGE to reach the optimum properties for a particular class of separations. All the models reviewed above have some serious limitations like considering only monovalent ions or neglecting the significant presence of H^+ or OH^- ions. The aim of the present paper is to introduce a mathematical and computational model that is as simple as possible to be easily used for optimization of the electrolyte systems for electrophoretic separation of anions. The model is limited neither to monovalent ions nor to the safe pH region and also allows for modeling of highly acidic or alkaline electrolytes. At maximum, the electrolyte can contain two co-anions and two counter-cations. It is the intention of this paper not only to formulate all necessary mathematical relations but also to show a concrete approach, the solution of which leads to the results.

In this section we will introduce the model and will demonstrate its suitability by inspecting the behavior of a commonly used phosphate buffer for analysis of anions. In the second section we will show a series of practical applications of the model for optimization of the BGEs in CZE.

2. Theory

The basic set-up of the model is similar to that proposed in Ref. [5] so, to keep the continuity, the symbols used generally correspond to those used there. The analyte can be a weak mono-, di- or trivalent acid X, which is co-migrating with two weak mono-, di- or trivalent acids of the BGE, A1 and A2. The two counter-ions can be weak mono-, di- or trivalent bases, B1 and B2. All those compounds, X, A1, A2, B1, B2, will be called components in the following text.

In order to have the notation as general as possible, we will suppose that chemical formulae of all the components, regardless of their attainable valency, will be formally always considered as trivalent electrolytes. Hence, the notation H_3X will be used for the neutral form of the analyte even if it were possibly only monovalent and existed only in the neutral form and the dissociated form, H_2X^-. The same rule will be applied for the anions A1, A2 and cations B1, B2 of the BGE.

All the components will be in acido–basic equilibria with their ionic forms: for analytes, they are H_2X^-, HX^{2-}, X^{3-}, background anions are H_2A1^-, $HA1^{2-}$, $A1^{3-}$ and H_2A2^-, $HA2^{2-}$, $A2^{3-}$, background cations are $B1H^+$, $B1H_2^{2+}$, $B1H_3^{3+}$ and $B2H^+$, $B2H_2^{2+}$, $B2H_3^{3+}$, respectively. It is thus obvious that every component in the system, X, A1, A2, B1, B2, can be present in four forms, one neutral and three ionic ones. The corresponding consecutive acidity constants will be denoted as: $K_{1,X}$, $K_{2,X}$, $K_{3,X}$ for the analyte, $K_{1,A1}$, $K_{2,A1}$, $K_{3,A1}$ and $K_{1,A2}$, $K_{2,A2}$, $K_{3,A2}$ for anions and $K_{1,B1}$, $K_{2,B1}$, $K_{3,B1}$ and $K_{1,B2}$, $K_{2,B2}$, $K_{3,B2}$ for cations, respectively. All the acidity constants are input parameters. It is allowed that the pH of the BGE is very low or very high, so the contribution of H^+ or OH^- ions for the transport of electric current will be taken into account.

The composition of the BGE consisting of A1, A2, B1, B2 and which forms a zone A, see Fig. 1, is supposedly completely known. The analyte X, in a very small concentration, migrates in the solution

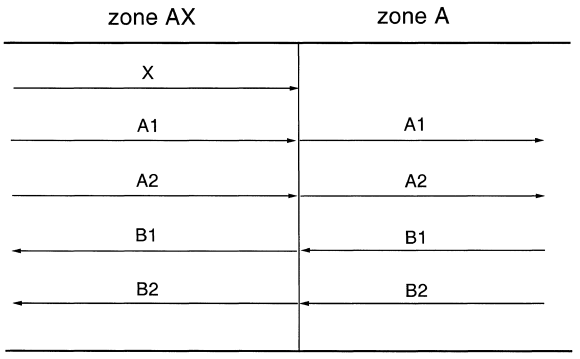

Fig. 1. Set-up of the electrolyte system. X, analyte; A1, A2, co-anions; B1, B2, counter-anions.

under influence of the electric field and forms the zone AX.

The analytical concentration of any component is a sum of concentrations of all its forms, both neutral and charged. The analytical concentrations will be denoted as $\bar{c}_{I,J}$, where subscripts denote Ith component in Jth zone. As the analytical composition of the BGE is known, the analytical concentrations $\bar{c}_{A1,A}$,$\bar{c}_{A2,A}$,$\bar{c}_{B1,A}$,$\bar{c}_{B2,A}$ in the zone A are regarded as input parameters. The present model neglects the influence of ionic strength on dissociation constants and mobilities. Thus, all activities will be approximated by the numerical values of the molar concentrations. The concentrations of all neutral and ionic forms in the zone A can be then easily calculated. One possible method of such calculation is shown in the Appendix.

The central point of the model is the evaluation of the composition of the BGE in the zone AX, or, in other words, the evaluation of a change in concentration of all its components, when a certain known and very small concentration of the sample, $\bar{c}_{X,AX}$, will reach the site of the detector by electrophoretic motion. This task brings a necessity to evaluate 21 concentrations: four forms of the four components of the BGE, three forms of the analyte (notice that the analytical concentration of the analyte, $\bar{c}_{X,AX}$, is the input parameter), plus H^+ and OH^- concentrations. Correspondingly, 21 equations have to be formulated.

The electroneutrality condition is a first equation, which puts all charged components into a relation. The acido–basic equilibria between neutral and charged forms in the solution are described by fifteen equations: three for each component X, A1, A2, B1, B2. The seventeenth equation is an equation for the water product K_W.

When neglecting diffusion and accepting that the movement of ions is caused only by the driving electric field, the mass balance at the boundary between A and AX zones leads to four equations sometimes called the moving boundary equations:

$$\bar{c}_{A1,A}(v_{A1,A} - v_{X,AX}) = \bar{c}_{A1,AX}(v_{A1,AX} - v_{X,AX}) \quad (1)$$

$$\bar{c}_{A2,A}(v_{A2,A} - v_{X,AX}) = \bar{c}_{A2,AX}(v_{A2,AX} - v_{X,AX}) \quad (2)$$

$$\bar{c}_{B1,A}(v_{B1,A} + v_{X,AX}) = \bar{c}_{B1,AX}(v_{B1,AX} + v_{X,AX}) \quad (3)$$

$$\bar{c}_{B2,A}(v_{B2,A} + v_{X,AX}) = \bar{c}_{B2,AX}(v_{B2,AX} + v_{X,AX}) \quad (4)$$

Here $v_{I,J}$ is the electrophoretic velocity of the Ith component in the Jth zone. In particular, $v_{X,AX}$ is the electrophoretic velocity of X in the zone AX, i.e. the velocity of the boundary between A and AX zones. All velocities are regarded as positive. The electrophoretic velocities $v_{I,J}$ are related to the effective mobilities $\bar{u}_{I,J}$ of the corresponding components in the corresponding zones by:

$$v_{I,J} = \bar{u}_{I,J} \cdot \frac{j}{\kappa_J} \quad (5)$$

where j is the electric current density and κ_J is the electric conductivity in the Jth zone. The knowledge of ionic mobilities of all charged forms in the solution enables to express the effective mobilities of the components and conductivities in the zones. All those ionic mobilities, $u_{K,L}$, where K denotes the ionic form and L denotes the component, are the input parameters of the model. Further, u_H and u_{OH} denote the ionic mobilities of hydrogen and hydroxide ions, respectively, and are also regarded as input parameters. Regardless of actual charge, all ionic mobilities will be considered as positive numbers. Due to the earlier stated approximation, all ionic mobilities are constants not dependent on ionic strength.

The above mathematical model eliminates the necessity of using the Kohlrausch regulating function, as it was used in the models by Gebauer et al. [15,22,29], which have been derived only for mono-

valent electrolytes. The detailed formulation of all equations of the mathematical model together with the approach for their solution is given in the Appendix.

Basically, the model provides information about the complete composition of the analyte zone AX, which will reach the detector. Of course, no detector is able to determine such a complete composition. For the indirect photometric detection the most decisive quantity responsible for detector signal is the slope of the dependence of the absorbance on the analyte concentration. However, regardless of the molar absorption coefficient of the components, the response of the concentration of co-ions (or sometimes counterions) on concentration of the analyte is of the primary importance. This quantity is the transfer ratio [10] which, in terms used in the present model, is defined as:

$$\mathrm{TR}_1 = \left(\frac{\mathrm{d}\bar{c}_{\mathrm{A1,AX}}}{\mathrm{d}\bar{c}_{\mathrm{X,AX}}}\right)_{\bar{c}_{\mathrm{X,AX}}\to 0},$$

$$\mathrm{TR}_2 = \left(\frac{\mathrm{d}\bar{c}_{\mathrm{A2,AX}}}{\mathrm{d}\bar{c}_{\mathrm{X,AX}}}\right)_{\bar{c}_{\mathrm{X,AX}}\to 0} \quad (6)$$

Analogously, conductivity detection is based on the change of BGE conductivity raised by the presence of the analyte. The corresponding quantity is called the molar conductivity detection response b_{X} [30] and is defined by:

$$b_{\mathrm{X}} = \left(\frac{\mathrm{d}\kappa_{\mathrm{AX}}}{\mathrm{d}\bar{c}_{\mathrm{X,AX}}}\right)_{\bar{c}_{\mathrm{X,AX}}\to 0} \quad (7)$$

where κ_{AX} is the conductivity in the zone AX.

The tendency of the sample peak to undergo electromigration dispersion is appropriately described by the velocity slope S_{X} [22]. Here we will use an analogous and more convenient form of this quantity, the relative velocity slope, which was proposed by Horká and Šlais [31]:

$$S_{\mathrm{X}} = \frac{\kappa_{\mathrm{AX}}}{v_{\mathrm{X,AX}}} \cdot \left(\frac{\mathrm{d}v_{\mathrm{X,AX}}}{\mathrm{d}\bar{c}_{\mathrm{X,AX}}}\right)_{\bar{c}_{\mathrm{X,AX}}\to 0} \quad (8)$$

The relative velocity slope has the same dimension as the molar conductivity response, i.e. S $\mathrm{m}^2/\mathrm{mol}$ in SI units. For strong ions it has even the same absolute value but the opposite sign. However, for weak electrolytes the value of the relative velocity slope generally has a different value than the molar conductivity response and can be higher or lower in the absolute value. The goal pursued in optimization of BGE's composition is finding electrolytes having a good signal and, at the same time, as low an electromigration dispersion as possible.

All quantities needed to fulfill such a task are defined in Eqs. (6)–(8) and can be easily obtained from the knowledge of the zone compositions of the AX zone. The input parameters for the optimization are $\mathrm{p}K_{\mathrm{a}}$ values and ionic mobilities of all compounds used and the composition of the BGE. Then, after finding suitable candidates, the real behavior of the system can be verified in practice. This way a usual trial-and-error experimental approach can be replaced by faster and more efficient computer simulation.

3. Experimental

3.1. Chemicals

Salicylic acid was provided by Sigma (St. Louis, MO, USA) phosphoric acid 85%, sodium chloride, sodium iodate were purchased from Lachema (Brno, Czech Republic); all chemicals were of analytical-reagent grade. Sodium hydroxide (0.1 *M*) was provided by Agilent Technologies (Waldbronn, Germany). Tetradecyltrimethylammonium hydroxide (TTAOH) was prepared from tetradecyltrimethylammonium bromide (Sigma) by ion-exchange on strongly basic ion exchanger Dowex 1 (Sigma). The water used for preparation of all the solutions was purified with a Milli-Q water purification system (Millipore, Bedford, MA, USA).

3.2. Instruments

All experiments were performed using the $\mathrm{HP}^{3\mathrm{D}}$CE capillary electrophoresis system (Agilent Technologies) equipped with a built-in photometric diode-array detection (DAD) system and a laboratory-made contactless conductivity detection (CCD) system [32]. The temperature was held at 25°C. Fused-silica capillary of 80 cm total length×75 μm I.D.×360 μm O.D., was used to carry out electrophoretic experiments. The distance from the injection

to detection points was 66 cm for the CCD system and 71.5 cm for the DAD system. The measuring wavelength of the DAD system was 200 nm. An injection of 100 mbar s and a separation voltage of −30 kV was employed for separation of the sample.

3.3. Computations

The solution of the mathematical model, which is described in the Appendix, was performed numerically using the Newton iteration method [33] which was applied for solving the sets of nonlinear equations. The computation algorithm was programmed both in Pascal and C++ languages using double-precision floating point operations. The input data used in the calculation for the electrolyte systems described are summarized in Table 1.

The calculated differential quantities, Eqs (6)–(8) are defined for an infinitely small concentration of the analyte. For the purpose of the calculation $c_{X,AX} = 5 \cdot 10^{-6}$ mol/m^3, i.e. $5 \cdot 10^{-6}$ mM was chosen as an approximation.

Table 1
Ionic mobilities, $u_{K,L}$, and negative logarithm of acidity constants, p$K_{K,L}$, of compounds used in calculation. Other constants used: ionic mobility of H^+ ions $u_H = 362.5 \cdot 10^{-9}$ m^2 V^{-1} s^{-1}, ionic mobility of OH^- ions $u_{OH} = 205.5 \cdot 10^{-9}$ m^2 V^{-1} s^{-1}, ionic product of water $K_w = 10^{-14}$

Component	$u_{K,L}$ (10^{-9} m^2 V^{-1} s^{-1})		p$K_{K,L}$	
Phosphoric acid	$u_{1,A1}$	34.6	p$K_{1,A1}$	2.16
	$u_{2,A1}$	61.4	p$K_{2,A1}$	7.21
	$u_{3,A1}$	71.5	p$K_{3,A1}$	12.67
Sodium hydroxide	$u_{1,B1}$	51.9	p$K_{1,B1}$	14
	$u_{2,B1}$	0	p$K_{2,B1}$	−10
	$u_{3,B1}$	0	p$K_{3,B1}$	−10
TTAOH	$u_{1,B2}$	25.0	p$K_{1,B2}$	14
	$u_{2,B2}$	0	p$K_{2,B2}$	−10
	$u_{3,B2}$	0	p$K_{3,B2}$	−10
Hydrochloric acid	$u_{1,X}$	79.1	p$K_{1,X}$	−2
	$u_{2,X}$	0	p$K_{2,X}$	20
	$u_{3,X}$	0	p$K_{3,X}$	20
Iodic acid	$u_{1,X}$	42.0	p$K_{1,X}$	0.77
	$u_{2,X}$	0	p$K_{2,X}$	20
	$u_{3,X}$	0	p$K_{3,X}$	20
Salicylic acid	$u_{1,X}$	35.4	p$K_{1,X}$	3.107
	$u_{2,X}$	0	p$K_{2,X}$	20
	$u_{3,X}$	0	p$K_{3,X}$	20

4. Results and discussion

The solution of the proposed model is a complete composition of the sample zone, when a sample with a certain very small concentration moves in the BGE under influence of the electric field. It would be rather complicated to depict all the 21 concentrations of all possible charged and neutral forms in the sample zone. Instead, the parameters of the system that are experimentally available, like the transfer ratio, molar conductivity detection response or effective mobility of analytes will be calculated.

A general suitability of the proposed model will be documented for inspection of properties of a generally utilized phosphate buffer, which is commonly used as a BGE with pH about 7 for separation of anions. In the particular buffer inspected here the cation of the buffers is Na^+ at 7.5 mM concentration and the cation of TTAOH at 0.1 mM concentration. TTAOH is used for the reversal of the electroosmotic flow. The anion is phosphate in concentration of 5 mM.

The results of the modeling will be shown in various forms. First it will be supposed that the sample is an arbitrary monovalent strong anion, which migrates in the buffer. The dependence of the differential quantities, Eqs (6)–(8), on the ionic mobility of this strong analyte anion will be shown in corresponding graphs. For S_X such a graph is in fact a depiction of one cut of the peak shape diagrams [22] for monovalent analytes with low p$K_{1,X}$. The graphs serve for inspection of a possible appearance of system peaks that are at the position of the singular point, where the parameters have a tendency to reach infinity. The acido–basic equilibrium responsible for buffering ability in the particular composition of the phosphate buffer is that between the doubly charged and the singly charged phosphates. As the calculated pH is 7.24 here, the presence of OH^- and H^+ ions is negligible. The behavior of this buffer is unexpected and highly interesting. Fig. 2 shows the molar conductivity response b_X, relative velocity slope S_X and transfer ratio TR_1 in their dependence on the ionic mobility of the analyte. The calculation gives a singularity at a mobility of about $42 \cdot 10^{-9}$ m^2 V^{-1} s^{-1}, which indicates a possible occurrence of the system peak with this mobility. It is thus obvious that even a

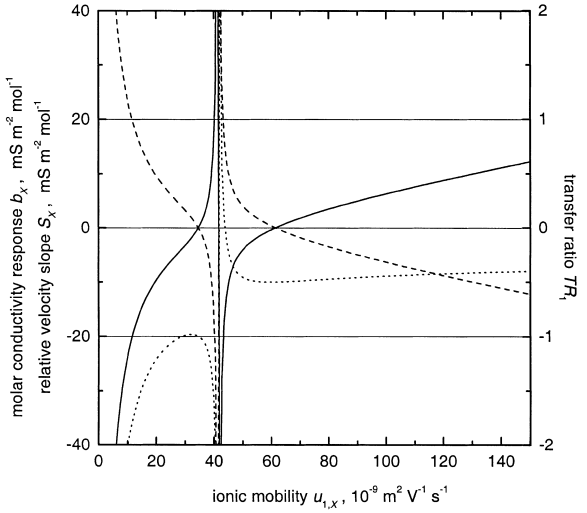

Fig. 2. Graph of the dependence of differential quantities on the ionic mobility of a strong monovalent analyte anion. Composition of the BGE: 5 m*M* phosphoric acid, 7.5 m*M* NaOH, 0.1 m*M* TTAOH; calculated pH 7.24. Solid line: b_X, molar conductivity detection response. Dashed line: S_X, relative velocity slope. Dotted line: TR_1, transfer ratio.

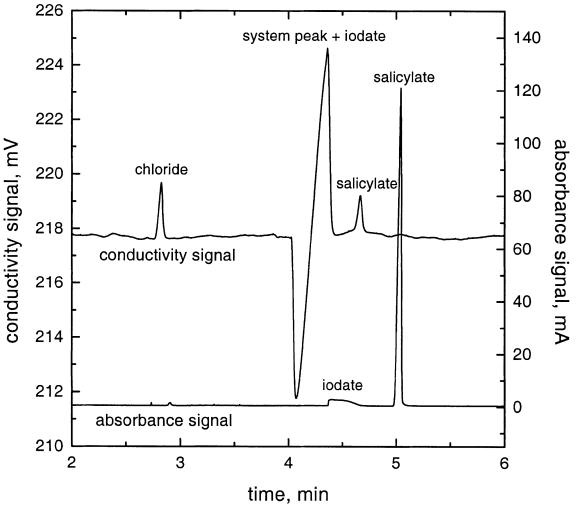

Fig. 3. Experimental record of the electrophoretic separation with CCD and DAD. Samples: chloride, iodate, salicylate, all at 1 m*M* concentration. Composition of the BGE: 5 m*M* phosphoric acid, 7.5 m*M* NaOH, 0.1 m*M* TTAOH; measured pH 7.1. Experimental: uncoated fused-silica capillary 80 cm (66 cm to the CCD system; 71.5 cm to the DAD system, measuring wavelength 200 nm) 75 μm I.D.×360 μm O.D., injection 100 mbar s; separation voltage −30 kV.

presence of two ionic forms ($H_2PO_4^-$ and HPO_4^{2-}) of a single component of the BGE causes the system to behave as a system with multiple co-ions giving the system eigenpeaks. Moreover, if a mobility of any analyte of the sample will be close to this value, the indirect detector signals following the BGE properties will be heavily amplified and distorted.

This behavior was confirmed in practice. Fig. 3 shows the experimental record of the electrophoretic separation using both a conductivity and photometric detection, when the sample is composed of hydrochloric acid, iodic acid and salicylic acid. As iodic acid is strong and its ionic mobility is $42.0 \cdot 10^{-9}$ $m^2\ V^{-1}\ s^{-1}$ which coincides with the mobility of the singularity, it should be expected that its conductivity signal will be extremely high and both positive and negative. The characteristic big zig-zag conductivity signal of iodic acid corresponds with these expectations. The photometric DAD system measuring the UV absorbance at 200 nm gives a different signal. As the UV absorbance of phosphates forming BGE and of chloride from the sample is negligible, only direct signals for iodate and salicylate should be expected. In accordance with the theoretical prediction, the signal of iodate is almost lost due to its excessive dispersion, while the salicylic acid still gives a nice, narrow peak.

The previous graphs would be difficult to draw, if the sample were a mixture of weak multivalent anions. Another output of the model is therefore a table giving the calculated effective mobility and differential quantities when the sample is separated in a given BGE. For the case inspected Table 2 presents the calculated effective mobility, molar conductivity response, relative mobility slope and transfer ratio for all analytes of the sample. For chloride and salicylate peaks the positive conductivity signal and fronting peak shape is forecasted, which is proved by the experiment. It is further obvious that although iodic acid has a very high molar conductivity response, $b_X = -72.25$ mS m^2 mol^{-1}, its relative mobility slope expressed by S_X is also very high, $S_X = 72.25$ mS m^2 mol^{-1}. It again means that the conductivity signal of the iodate peak will be big and dispersed.

Naturally, phosphate buffers of varying buffering capacity can be prepared for an arbitrary pH. To describe the behavior of such phosphate buffers it

Table 2
Calculated parameters of the analytes when separated in phosphate buffer (5 m*M* phosphoric acid, 7.5 m*M* NaOH, 0.1 m*M* TTAOH, calculated pH 7.24)

Component	Effective mobility $\bar{u}_{X,AX}$ (10^{-9} m^2 V^{-1} s^{-1})	Molar conductivity response b_X (mS m^2 mol^{-1})	Relative mobility slope S_X (mS m^2 mol^{-1})	Transfer ratio TR_1
Hydrochloric acid	79.1	3.345	−3.345	−0.475
Iodic acid	42.0	−72.25	72.25	2.818
Salicylic acid	35.4	0.791	−0.788	−1.017

should be useful to show the dependence of the particular quantities on the composition or pH of the buffer. The critical feature of the electrolytes used for CZE is the appearance of the system peaks, the mobilities of which correspond with singular points of the $S_X - u_X$ or $b_X - u_X$ dependence. An example of such a graph, which can be called the electrolyte performance diagram (EPD) is shown in Fig. 4. This is a two dimensional diagram for S_X, which is represented by a hue in the grayscale. The diagram is sort of a generalization of the previous diagram in Fig. 2: here the S_X is depicted in its dependence both on the composition of the background buffer and the mobility of a strong analyte. The values of S_X close to zero are represented as a neutral or gray hue. Such areas have low electromigration dispersion. Positive and negative values of S_X attain gradually brighter and darker hues, respectively. The presence of the singularities is indicated by sharp ridges on the picture, where both white and black colors touch together. The first ridge of an S-shape at concentration of phosphoric acid of 4–7 m*M* denotes the presence of the system peak due to the concurrent presence of the $H_2PO_4^-$ and HPO_4^{2-} ions. The second ridge at concentration of 3–4 m*M* indicates a fast system peak with mobilities of about $160 \cdot 10^{-9}$–$180 \cdot 10^{-9}$ m^2 V^{-1} s^{-1} due to the significant presence of OH^- ions. If the mobilities of analyzed ions are close to such singularities, their movement coincides with the movement of the system peaks and the analytes are buried within them due to the severe dispersion. Such phenomena can disturb many practical separations.

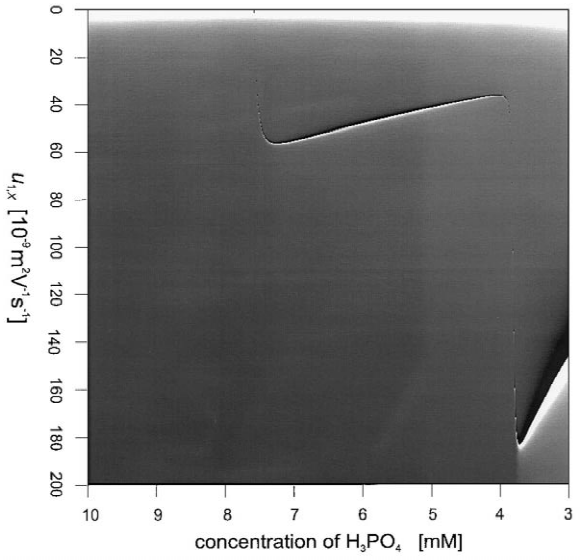

Fig. 4. Electrolyte performance diagram. Dependence of S_X on composition of phosphate buffer and mobility $u_{1,X}$ of a strong monovalent analyte. Composition of the buffer: 7.5 m*M* NaOH, 0.1 m*M* TTAOH, concentration of phosphoric acid is at the vertical axis. S_X is represented in the grayscale: $S=0$ gray hue, $S>0$ brighter grade, $S<0$ darker grade.

5. Concluding remarks

When trying to find optimum BGE composition, it should be a general intention to reach the maximum values of the quantities expressing sensitivity of detection. On the other hand, the relative velocity slope S_X is a quantity which should be kept small in the absolute value as it describes the tendency of the analyte to undergo electromigration dispersion. The ideal situation is when $S_X = 0$, which means that the electromigration dispersion does not take place even at a finite analyte concentration. Such a situation can be arranged in electrophoresis with direct or indirect photometric detection: when choosing a co-ion with the same velocity as the velocity of the analyte. Unfortunately, this arrangement is not functional in electrophoresis with conductivity detection: when the velocity (or mobility) of the co-ion is the same as

that of the analyte, the detection response $b_X = 0$ and the conductivity detector does not provide any signal. Finding a suitable electrolyte system when using conductivity detection is therefore a matter of compromise: the mobility of the co-ion has to be different from the mobility of the analyte to get the conductivity signal, nevertheless, the electrolyte systems should be chosen to cause as small an electromigration dispersion as possible. Both the theory and practice show that such electrolytes can be found. This will be documented in the subsequent part of this series.

Although the model presented here is aimed for separation of anions in electrolytes containing two trivalent co-ions and two trivalent counter-ions at maximum, it can be straightforwardly rearranged to serve for simulation of electromigration of cationic analytes. Additionally, it can be uncomplicatedly generalized for higher number of ions having a higher valency than three.

Acknowledgements

The support of the research grant by the Ministry of Education of the Czech Republic, grant No. J13/98:113100001 is gratefully acknowledged.

Appendix

Composition in zone A: BGE

The analytical concentrations of all components of the BGE, $\bar{c}_{A1,A}$,$\bar{c}_{A2,A}$,$\bar{c}_{B1,A}$,$\bar{c}_{B2,A}$, are input parameters.

For the purposes of brevity, short symbols *Di*, $i = 1,..,14$ in the following text stand for concentration of the appropriate ionic forms in zone A:

Symbol	Form	Symbol	Form
$D1$	H^+	$D8$	$B1H^+$
$D2$	H_2A1^-	$D9$	$B1H_2^{2+}$
$D3$	$HA1^{2-}$	$D10$	$B1H_3^{3+}$
$D4$	$A1^{3-}$	$D11$	$B2H^+$
$D5$	H_2A2^-	$D12$	$B2H_2^{2+}$
$D6$	$HA2^{2-}$	$D13$	$B2H_3^{3+}$
$D7$	$A1^{3-}$	$D14$	OH^-

The fourteen equations enabling the calculation of all the concentrations of all ionic forms are as follows:

$$
\begin{aligned}
0 &= D1 - D2 - 2D3 - 3D4 - D5 - 2D6 - 3D7 \\
&\quad + D8 + 2D9 + 3D10 + D11 + 2D12 + 3D13 \\
&\quad - D14 \\
0 &= K_{1,A1}(\bar{c}_{A1,A} - D2 - D3 - D4) - D1D2 \\
0 &= K_{2,A1}D2 - D1D3 \\
0 &= K_{3,A1}D3 - D1D4 \\
0 &= K_{1,A2}(\bar{c}_{A2,A} - D5 - D6 - D7) - D1D5 \\
0 &= K_{2,A2}D5 - D1D6 \\
0 &= K_{3,A2}D6 - D1D7 \\
0 &= K_{1,B1}D8 - (\bar{c}_{B1,A} - D8 - D9 - D10)D1 \\
0 &= K_{2,B1}D9 - D1D8 \\
0 &= K_{3,B1}D10 - D1D9 \\
0 &= K_{1,B2}D11 - (\bar{c}_{B2,A} - D11 - D12 - D13)D1 \\
0 &= K_{2,B2}D12 - D1D11 \\
0 &= K_{3,B2}D13 - D1D12 \\
0 &= D1D14 - K_w
\end{aligned}
\qquad \text{(A.1)}
$$

The first equations express the electroneutrality condition; all the following equations describe acido–basic equilibria.

What is convenient to evaluate for subsequent evaluation of the zone AX are conductivity κ_A of zone A:

$$
\begin{aligned}
\kappa_A = F(&u_H D1 + u_{1,A1}D2 + 2u_{2,A1}D3 + 3u_{3,A1}D4 \\
&+ u_{1,A2}D5 + 2u_{2,A2}D6 + 3u_{3,A2}D7 \\
&+ u_{1,B1}D8 + 2u_{2,B1}D9 + 3u_{3,B1}D10 + u_{1,B2}D11 \\
&+ 2u_{2,B2}D12 + 3u_{3,B2}D13 + u_{OH}D14)
\end{aligned}
\qquad \text{(A.2)}
$$

and products:

$$
\begin{aligned}
\bar{c}_{A1,A}\bar{u}_{A1,A} &= u_{1,A1}D2 + u_{2,A1}D3 + u_{3,A1}D4 \\
\bar{c}_{A2,A}\bar{u}_{A2,A} &= u_{1,A2}D5 + u_{2,A2}D6 + u_{3,A2}D7 \\
\bar{c}_{B1,A}\bar{u}_{B1,A} &= u_{1,B1}D8 + u_{2,B1}D9 + u_{3,B1}D10 \\
\bar{c}_{B2,A}\bar{u}_{B2,A} &= u_{1,B2}D11 + u_{2,B2}D12 + u_{3,B2}D13
\end{aligned}
\qquad \text{(A.3)}
$$

Here, F is the Faraday constant.

Composition in zone AX: sample zone

Analogously to the previous zone A, the symbols *Ei*, $i=1,..,21$, stand for concentration of the appropriate ionic forms or analytical concentrations in the zone AX:

Symbol	Form	Symbol	Form
$E1$	H^+	$E14$	H_2X^-
$E2$	H_2A1^-	$E15$	HX^{2-}
$E3$	$HA1^{2-}$	$E16$	X^{3-}
$E4$	$A1^{3-}$	$E17$	$H_3A1+H_2A1^-+HA1^{2-}+A1^{3-}=\bar{c}_{A1,AX}$
$E5$	H_2A2^-	$E18$	$H_3A2+H_2A2^-+HA2^{2-}+A2^{3-}=\bar{c}_{A2,AX}$
$E6$	$HA2^{2-}$	$E19$	$B1+B1H^+ +B1H_2^{2+}+B1H_3^{3+}=\bar{c}_{B1,AX}$
$E7$	$A1^{3-}$	$E20$	$B2+B2H^+ +B2H_2^{2+}+B2H_3^{3+}=\bar{c}_{B2,AX}$
$E8$	$B1H^+$	$E21$	OH^-
$E9$	$B1H_2^{2+}$		
$E10$	$B1H_3^{3+}$		
$E11$	$B2H^+$		
$E12$	$B2H_2^{2+}$		
$E13$	$B2H_3^{3+}$		

The electroneutrality condition and acidobasic equilibria are expressed here as:

$$
\begin{aligned}
0 &= E1 - E2 - 2E3 - 3E4 - E5 - 2E6 - 3E7 \\
&\quad + E8 + 2E9 + 3E10 + E11 + 2E12 + 3E13 \\
&\quad - E14 - 2E15 - 3E16 - E21 \\
0 &= K_{1,A1}(E17 - E2 - E3 - E4) - E1E2 \\
0 &= K_{2,A1}E2 - E1E3 \\
0 &= K_{3,A1}E3 - E1E4 \\
0 &= K_{1,A2}(E18 - E5 - E6 - E7) - E1E5 \\
0 &= K_{2,A2}E5 - E1E6 \\
0 &= K_{3,A2}E6 - E1E7 \\
0 &= K_{1,B1}E8 - (E19 - E8 - E9 - E10)E1 \\
0 &= K_{2,B1}E9 - E1E8 \\
0 &= K_{3,B1}E10 - E1E9 \\
0 &= K_{1,B2}E11 - (E20 - E11 - E12 - E13)E1 \\
0 &= K_{2,B2}E12 - E1E11 \\
0 &= K_{3,B2}E13 - E1E12 \\
0 &= K_{1,X}(\bar{c}_{X,AX} - E14 - E15 - E16) - E1E14 \\
0 &= K_{2,X}E14 - E1E15 \\
0 &= K_{3,X}E15 - E1E16 \\
0 &= E1E21 - K_w
\end{aligned}
\qquad \text{(A.4)}
$$

When rewriting Eqs. (1)−(4) by means of Eq. (5) and using ionic mobilities instead of effective mobilities, the following four equations result:

$$
\begin{aligned}
0 &= \kappa_{AX}\bar{c}_{A1,A}\bar{u}_{A1,A} - \kappa_A \cdot \Big[u_{1,A1}E2 + u_{2,A1}E3 + u_{3,A1}E4 \\
&\quad + \bar{c}_{A1,A} \cdot \frac{u_{1,X}E14 + u_{2,X}E15 + u_{3,X}E16}{\bar{c}_{X,AX}} \\
&\quad - E17 \cdot \frac{u_{1,X}E14 + u_{2,X}E15 + u_{3,X}E16}{\bar{c}_{X,AX}} \Big] \\
0 &= \kappa_{AX}\bar{c}_{A2,A}\bar{u}_{A2,A} \\
&\quad - \kappa_A \cdot \Big[u_{1,A2}E5 + u_{2,A2}E6 + u_{3,A2}E7 \\
&\quad + \bar{c}_{A2,A} \cdot \frac{u_{1,X}E14 + u_{2,X}E15 + u_{3,X}E16}{\bar{c}_{X,AX}} \\
&\quad - E18 \cdot \frac{u_{1,X}E14 + u_{2,X}E15 + u_{3,X}E16}{\bar{c}_{X,AX}} \Big] \\
0 &= \kappa_{AX}\bar{c}_{B1,A}\bar{u}_{B1,A} \\
&\quad - \kappa_A \cdot \Big[u_{1,B1}E8 + u_{2,B1}E9 + u_{3,B1}E10 \\
&\quad + E19 \cdot \frac{u_{1,X}E14 + u_{2,X}E15 + u_{3,X}E16}{\bar{c}_{X,AX}} \\
&\quad - \bar{c}_{B1,A} \cdot \frac{u_{1,X}E14 + u_{2,X}E15 + u_{3,X}E16}{\bar{c}_{X,AX}} \Big] \\
0 &= \kappa_{AX}\bar{c}_{B2,A}\bar{u}_{B2,A} \\
&\quad - \kappa_{rA} \cdot \Big[u_{1,B2}E11 + u_{2,B2}E12 + u_{3,B2}E13 \\
&\quad + E20 \cdot \frac{u_{1,X}E14 + u_{2,X}E15 + u_{3,X}E16}{\bar{c}_{X,AX}} \\
&\quad - \bar{c}_{B2,A} \cdot \frac{u_{1,X}E14 + u_{2,X}E15 + u_{3,X}E16}{\bar{c}_{X,AX}} \Big]
\end{aligned}
\qquad \text{(A.5)}
$$

where the conductivity κ_{AX} of the AX zone is:

$$
\begin{aligned}
\kappa_{AX} &= F(u_H E1 + u_{1,A1} + E2 + 2u_{2,A1}E3 + 3u_{3,A1}E4 \\
&\quad + u_{1,A2}E5 + 2u_{2,A2}E6 + 3u_{3,A2}E7 \\
&\quad + u_{1,B1}E8 + 2u_{2,B1}E9 + 3u_{3,B1}E10 + u_{1,B2}E11 \\
&\quad + 2u_{2,B2}E12 + 3u_{3,B2}E13 + u_{1,X}E14 \\
&\quad + 2u_{2,X}E15 + 3u_{3,X}E16 + u_{OH}E21)
\end{aligned}
\qquad \text{(A.6)}
$$

Computer calculation

Solution of the above sets of the nonlinear equations was performed by the Newton iteration method.

The set of Eqs. (A.1) is solved first which gives all Di, $D1, \ldots, D14$. Consequently some auxiliary quantities, Eqs. (A2) and (A3) are enumerated. The second step is the solution of the set of 21 equations, Eqs.(A4) and (A5), the result of which are values of all Ei, $E1, \ldots, E21$.

The differential quantities can be calculated as:

$$b_X = \frac{\kappa_{AX} - \kappa_A}{\bar{c}_{X,AX}} \tag{A.7}$$

$$TR_1 = \frac{E17 - \bar{c}_{A1,A}}{\bar{c}_{X,AX}}, TR_2 = \frac{E18 - \bar{c}_{A2,A}}{\bar{c}_{X,AX}} \tag{A.8}$$

$$S_X = \frac{\kappa_A}{v_{X,A}}\left(\frac{v_{X,AX} - v_{X,A}}{\bar{c}_{X,AX}}\right) \tag{A.9}$$

The velocity $v_{X,AX}$ of X in the zone AX is expressed as:

$$v_{X,AX} = \frac{i(u_{1,X}E14 + u_{2,X}E15 + u_{3X}E16)}{F\bar{c}_{X,AX}\kappa_{AX}} \tag{A.10}$$

and the hypothetical velocity $v_{X,A}$ in the zone A is:

$$v_{X,A} = \frac{i}{F\kappa_A}\left(\frac{u_{1,X}}{D1/K_{1,X} + 1 + K_{2,X}/D1 + K_{2,X}K_{3,X}/D1^2} + \frac{u_{2,X}}{D1^2/(K_{1,X}K_{2,X}) + D1/K_{2,X} + 1 + K_{3,X}/D1} + \frac{u_{3,X}}{D1^3/(K_{1,X}K_{2,X}K_{3,X}) + D1^2/(K_{2,X}K_{3,X}) + D1/K_{3,X} + 1}\right) \tag{A.11}$$

The current density i cancels when calculating S_X by Eq. (A.9).

References

[1] V. Pacáková, P. Coufal, K. Štulík, J. Chromatogr. A 834 (1999) 257.
[2] P. Doble, P.R. Haddad, J. Chromatogr. A 834 (1999) 189.
[3] H. Poppe, J. Chromatogr. 506 (1990) 45.
[4] H. Poppe, Anal. Chem. 64 (1992) 1908.
[5] J.L. Beckers, J. Chromatogr. A 662 (1994) 153.
[6] J.L. Beckers, J. Chromatogr. A 679 (1994) 153.
[7] P. Gebauer, P. Boček, J. Chromatogr. A 772 (1997) 73.
[8] C. Desiderio, S. Fanali, P. Gebauer, P. Boček, J. Chromatogr. A 772 (1997) 81.
[9] M. Macka, P.R. Haddad, P. Gebauer, P. Boček, Electrophoresis 18 (1997) 1998.
[10] J.L. Beckers, J. Chromatogr. A 844 (1999) 321.
[11] R.L. Williams, B. Childs, E.V. Dose, G. Guiochon, G. Vigh, Anal. Chem. 69 (1997) 1347.
[12] R.L. Williams, B. Childs, E.V. Dose, G. Guiochon, G. Vigh, J. Chromatogr. A 781 (1997) 107.
[13] P. Gebauer, C. Desiderio, S. Fanali, P. Boček, Electrophoresis 19 (1998) 701.
[14] P. Doble, P.R. Haddad, Anal. Chem. 71 (1999) 15.
[15] P. Gebauer, P. Borecká, P. Boček, Anal. Chem. 70 (1998) 3397.
[16] P. Boček, P. Gebauer, J. Beckers, in: presented at the 13th International Symposium on High Performance Capillary Electrophoresis and Related Microscale Techniques, Saarbrücken, 20–24 February, 2000, p. 144, Abstracts.
[17] F.M. Everaerts, J.L. Beckers, Th.P.E.M. Verheggen, Isotachophoresis — Theory, Instrumentation and Application, Elsevier, Amsterdam, Oxford, New York, 1976.
[18] J.L. Beckers, J. Chromatogr. A 693 (1995) 347.
[19] J.L. Beckers, J. Chromatogr. A 696 (1995) 285.
[20] J.L. Beckers, J. Chromatogr. A 741 (1996) 265.
[21] J.L. Beckers, J. Chromatogr. A 764 (1997) 111.
[22] P. Gebauer, P. Boček, Anal. Chem. 69 (1997) 1557.
[23] P. Gebauer, J. Čáslavská, W. Thormann, P. Boček, J. Chromatogr, A 772A (1997) 63.
[24] X. Xiong, S.F.Y. Li, J. Chromatogr. A 835 (1999) 169.
[25] F.E.P. Mikkers, Anal. Chem. 71 (1999) 522.
[26] F. Kohlrausch, Ann. Phys. {Leipzig) 62 (1897) 209.
[27] S.V. Ermakov, M.Y. Zhukov, L. Capelli, P.G. Righetti, Electrophoresis 19 (1998) 192.
[28] B. Gaš, J. Vacík, I. Zelenský, J. Chromatogr. 545 (1991) 225.
[29] P. Gebauer, P. Pantucková, P. Boček, Anal. Chem. 71 (1999) 3374.
[30] F.E.P. Mikkers, F.M. Everaerts, Th.P.E.M. Verheggen, J. Chromatogr. 169 (1979) 1.
[31] M. Horká, K. Šlais, Electrophoresis 21 (2000) 2814.
[32] B. Gaš, P. Coufal, J. Zuska, in: Presented at the 13th International Symposium on High-Performance Capillary Electrophoresis and Related Microscale Techniques, Saarbrücken, 20–24 February, 2000, p. 134, Abstracts.
[33] A. Ralston, A First Course in Numerical Methods, McGraw-Hill, New York, 1965.